Proc. of the 2018 International Symposium on Electromagnetic Compatibility (EMC Europe 2018), Amsterdam, The Netherlands, August 27−30, 2018.

Plane Wave Spectrum Method Applied on Radiated Magnetic Field from RFID Reader Antenna

Kassem Jomaa*, Fabien Ndagijimana
IMEP-LaHC Laboratory
Grenoble-Alpes University
Grenoble, France
*kassem.jomaa@minatec.grenoble-inp.fr

Hussam Ayad, Majida Fadlallah, and Jalal Jomaah
Physics Department, Faculty of Sciences
Lebanese University
Beirut, Lebanon

***Abstract*—Near electromagnetic field characterization for radiating devices requires the 3D field mapping in the space near this device, especially for dosimetric applications. In this work we present the plane wave spectrum (PWS) method to extract the 3D magnetic field components from the transverse ones, in addition to the extraction of the filed at different planes above the device under test (DUT). This operation was performed on an RFID reader antenna operating at 13.56 MHz that was designed and simulated on HFSS (high frequency structural simulator). Good agreements were found by comparing the theoretical, simulated, and extracted magnetic field quantities at different heights.**

***Keywords* — Electromagnetic compatibility, radiation, near-field, magnetic field, plane wave spectrum.**

I. INTRODUCTION

Near field characterization is a challenging process in electromagnetic compatibility studies. Several approaches have been proposed to achieve the required scanning of the radiating source throughout the space. Radiated emission and immunity tests of electronic circuits are important tasks of system electromagnetic compatibility analysis and they have become growing concerns in prediction of system reliability [1]-[3]. Also for dosimetric applications it is necessary to have a 3D field mapping in the vicinity of the radiating source. In this context, several near-field scanning systems were introduced [4]-[6]. In a previous work, we introduced a three axis magnetic field probes [7]. The 3 components of the magnetic field can then be measured simultaneously with a single planner scan above the DUT. For dosimetric studies, the field distribution in the near-field region needs to be known. Hence several scans should be done in order to build the 3D field mapping, and this leads to time consuming. For this reason it is better to find an analytical solution that reduces the number of scans needed. The PWS approach has been found useful for determining the far field from near field measurements [8][9]. The reconstruction algorithm requires just the 2D scan of the tangential components to reconstruct the 3D magnetic field distribution.

In this paper the near field characterization is performed on an RFID reader antenna. The PWS method is applied to extract the three components of the magnetic field in the near field region at different planes from the tangential components at a plane near the radiating source. The RFID rectangular loop antenna operating at 13.56 MHz was modeled on MATLAB and simulated on HFSS. The theoretical calculations of the magnetic field profile at different planes above the antenna were performed and compared, with the simulated ones, to the extracted values from the PWS method.

II. PLANE WAVE SPECTRUM METHOD

Electromagnetic fields can be represented as plane waves propagating in the space in all directions and with different amplitudes. PWS transformation allows the decomposition of the electromagnetic field components mapped in a plan as being the sum of 2D harmonic spectrums of the propagating plane waves. Hence the knowledge of the transverse field components over a plane near a radiating antenna can be used to extract the plane wave spectrum of the radiated electromagnetic fields. Plane waves satisfy Helmholtz equation given by:

$$\nabla^2 \vec{A} + k^2 \vec{A} = 0 \tag{1}$$

where $\vec{A}$ is the field quantity vector, which can be either electric or magnetic field, and k is the wavenumber.

A general solution of (1) can be:

$$\vec{A}(\vec{r}) = \vec{F_A}(\vec{k}) e^{-j\vec{k}\vec{r}} \tag{2}$$

where $\vec{k}$ is the wave vector, given by:

$$\vec{k} = k_x \vec{u_x} + k_y \vec{u_y} + k_z \vec{u_z}$$

$$k = \sqrt{k_x^2 + k_y^2 + k_z^2} = \omega\sqrt{\mu\varepsilon} \ ,$$

$\vec{r}$ is the position vector, expressed by:

$$\vec{r} = x\vec{u_x} + y\vec{u_y} + z\vec{u_z} \ ,$$

and $\vec{F_A}$ is the plane wave spectrum vector of the field $\vec{A}$.

From the wave vector relation one can notice that knowing the frequency and two of the components it is possible to calculate the third one. Assuming that the direction of propagation is along $\vec{u_z}$ direction, the transverse field components will be in the ***xy*** plane, so we can obtain by the following:

$$k_z = \begin{cases} \sqrt{k^2 - k_x^2 - k_y^2} & if \quad k^2 \geq k_x^2 + k_y^2 \\ -i\sqrt{k_x^2 + k_y^2 - k^2} & other \end{cases}$$

In this paper, we will work on the magnetic field quantity. The solution of the Helmholtz equation (1) could be determined by Fourier transform method that leads to a solution expressed in terms of the plane wave spectrum [10]. Therefore, the complex vector $\vec{F_h}(k_x,k_y)$ will be taken as the plane wave spectrum of the transverse magnetic field components and it is expressed by:

$$\vec{F_h}(k_x,k_y)=\int_{-\infty}^{+\infty}\int_{-\infty}^{+\infty}\vec{H}(x,y)e^{j(k_x x+k_y y)}dxdy \qquad (3)$$

By applying (3) to the magnetic field components $\boldsymbol{H_x}$ and $\boldsymbol{H_y}$ at $\boldsymbol{P_0}$ we can obtain the plane wave spectrum components $\boldsymbol{F_{hx}}$ and $\boldsymbol{F_{hy}}$. Moreover, by substituting (2) in Guess's law for magnetism from Maxwell's equations:

$$\nabla.\vec{H}=0 \qquad (4)$$

we can find a relation between the three spectral components of the magnetic field:

$$\vec{k}.\vec{F_h}=0$$

$$k_xF_{hx}+k_yF_{hy}+k_zF_{hz}=0$$

$$F_{hz}=-\frac{k_xF_{hx}+k_yF_{hy}}{k_z} \qquad (5)$$

The magnetic field component $\boldsymbol{H_z}$ can then be reconstructed from (5) by using the inverse of the plane wave spectrum (IPWS) method:

$$\vec{H}_z=\frac{1}{4\pi^2}\int_{-\infty}^{+\infty}\int_{-\infty}^{+\infty}\vec{F_{hz}}(k_x,k_y)e^{-j(k_x x+k_y y)}dk_xdk_y \qquad (6)$$

Moreover the spectral components of the magnetic field at different highs above the plane $\boldsymbol{P_0}$ can be obtained from the spectral components at $\boldsymbol{z_0}$ by the following relationship:

$$F_h(\mathrm{z})=F_h(\mathrm{z}_0)\,\mathrm{e}^{-jk_z(\mathrm{z}-\mathrm{z}_0)} \qquad (7)$$

The magnetic field components at height $\boldsymbol{z}$ can then be calculated by IPWS method as in (6). In the near field region the plane $\boldsymbol{P_0}$ at a height $\boldsymbol{z_0}$ above the DUT should satisfy the following relation:

$$z_0<\frac{\lambda}{2\pi} \qquad (8)$$

where $\boldsymbol{\lambda}$ is the wavelength of the signal at the operating frequency $\boldsymbol{f}$. Fig. 1 summarizes the whole process of the PWS algorithm and its inverse showing the spatial and spectral components.

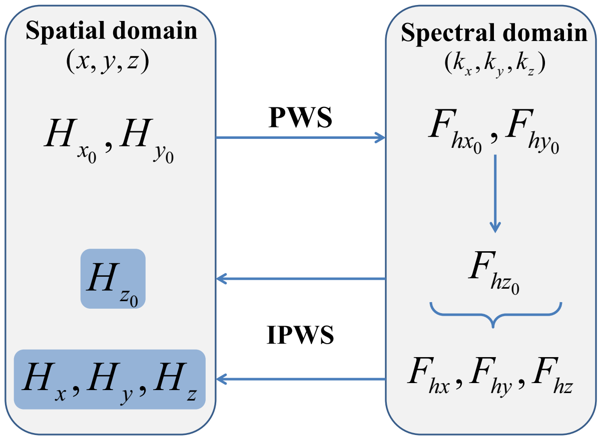

Fig. 1. PWS method for magnetic field extraction

III. RFID Reader Antenna

A. Loop Antennas

RFID readers are designed with loop antennas, which feature simplicity, low cost and versatility. They are made of a loop with a conductor that may have various shapes: circular, rectangular, triangular, elliptical, etc. They are widely used in communication links up to the microwave bands and also as electromagnetic field probes.

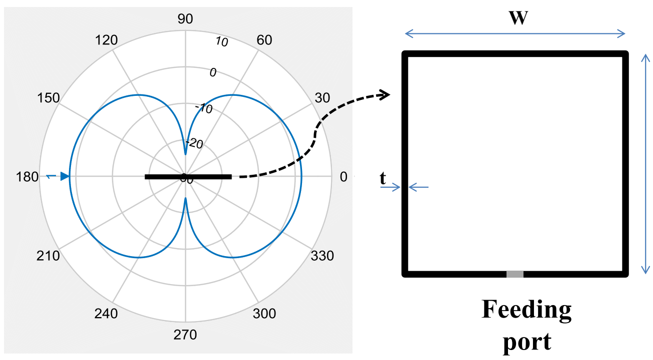

Fig. 2. Single turn rectangular loop antenna with the corresponding radiation pattern diagram

Loop antennas are usually classified as electrically small and electrically large loop antennas. Electrically small loop antennas are those who have their circumference $\boldsymbol{C}$ less than tenth of the wavelength ($\boldsymbol{C} < 0.1\lambda$), while in electrically large antennas the circumference is near the wavelength ($\boldsymbol{C} \approx \lambda$). Small loop antennas are equivalent to a magnetic dipole and they have a far-field radiation pattern very similar to that of a small electric dipole normal to the plane of the loop as shown in Fig. 2. [11].

B. Antenna Under Test

In this work, a rectangular small loop antenna operating at 13.56 MHz was modeled on MATLAB and simulated on HFSS in order to test the PWS algorithm. It is the typical RFID reader antenna used in library RFID systems [12]. The antenna was modelled on MATLAB based on the theoretical formulations loop antennas given in [11]. The loop has a length L=140mm, width W=140mm and a copper trace thickness t=5mm. The feeding point is at the center of one of the sides. The antenna is excited by a time-harmonic voltage signal with the amplitude of 1 V and a frequency of 13.56 MHz at the feeding port. The HFSS designed structure is shown in Fig. 3 including three different planes above the antenna at heights of 1, 5, and 10 centimeters and with 2D dimensions of L_x = 40cm and L_y = 40cm. The three magnetic field components H_x, H_y, and H_z are exported at these planes with a grid size of 10mm. In order to obtain high accuracy in the exported data, the planes are meshed by a length based operation with a maximum length of 10mm.

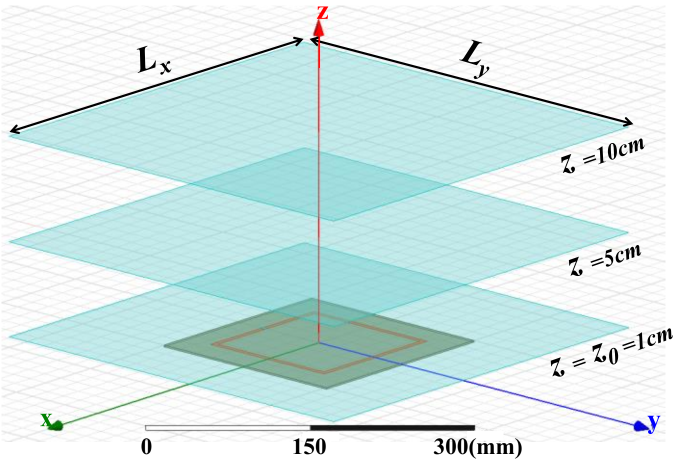

Fig. 3. RFID Loop Antenna structure

IV. RESULTS AND DISCUSSION

The numerical execution of the PWS algorithm is performed on the data obtained from the simulated structure and it is then compared to the theoretical ones. The initial input parameters for the numerical calculations are:

- the tangential H-field components, H_x & H_y
- the spatial parameters: L_x, L_y, Δx, and Δy
- the wavelength λ that is $\lambda = c / f$

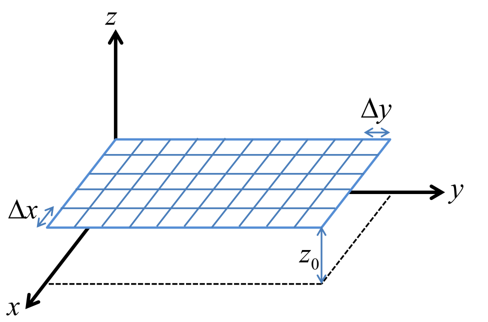

Fig. 4. Spatial domain parameters representing the plane P_0 at $z=z_0$

The plane P_0 is at height z_0=1cm above the DUT and have the dimensions of $L_x \times L_y$ with $L_x = L_y$ = 40cm. The plane is discretized in both x & y axis with an equal step size of $\Delta x = \Delta y$ = 10mm. The discrete indices along these two axes are n_x & n_y respectively:

$$n_x = \frac{L_x}{\Delta x} \quad ; \quad n_y = \frac{L_y}{\Delta y}$$

The discretized tangential wave vector components used in the numerical computation are calculated using the following formulas:

$$\Delta k_x = \frac{2\pi}{L_x} \quad ; \quad \Delta k_y = \frac{2\pi}{L_y}$$

The spatial and discretization parameters should be chosen according to the following condition:

$$Max\left(\Delta k_x, \Delta k_y\right) < \frac{2\pi}{\lambda}$$

The first step in the proposed algorithm is to obtain the normal magnetic field H_z from the tangential components. As introduced in section II, this occurs by calculating the plane wave spectrum of the tangential components using (3), and then by applying (5) we obtain the normal spectral component of the magnetic field F_{hz}, after that H_z is reconstructed with the inverse of PWS as stated in (6). The results are shown in Fig. 5; it shows the theoretical, simulated, and the calculated magnitudes of H_z. It is clear that the reconstructed filed is in good agreement with the theoretical one.

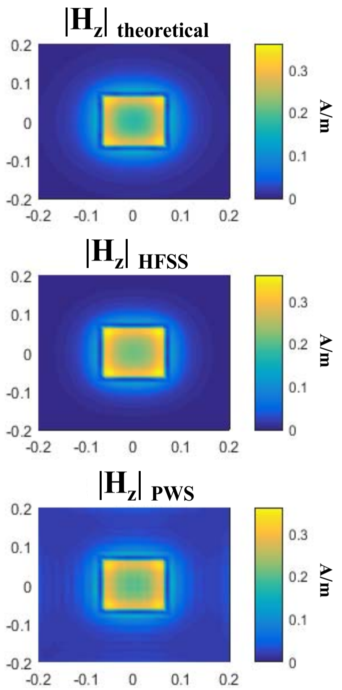

Fig. 5. Comparison between theoretical, simulated, and calculated values of the H_z magnetic field component at P_0

The other part of the PWS method is to extract the field components at different planes in the space above the DUT just from the field quantities in a single plane near the radiation source. By applying (7) we can obtain the spectral components of the magnetic field at the needed height z. Then by performing IPWS we can have the magnetic field at this height. In RFID near-field characterization, we aim to study the field levels in the near-field region in order to see the dosimetric levels of the radiated magnetic field. For this reason we would chose 2 planes that relay in the normal region of operation of the RFID systems. We chose the plane $\boldsymbol{P_1}$ and $\boldsymbol{P_2}$ that are respectively at 5 and 10 centimeters above the reader antenna. Then the reconstruction algorithm is applied based on the magnetic field quantities at $\boldsymbol{P_0}$. The results are shown in Fig. 6 and Fig. 7, good agreement can also be found by comparing the theoretical, simulated, and extracted magnetic field profiles at the chosen planes $\boldsymbol{P_1}$ and $\boldsymbol{P_2}$. We can observe a little noisy profile in the normal extracted magnetic field $\boldsymbol{H_z}$ at the edges of the computed area; this could be solved by adding zero padding to the initial data at $\boldsymbol{P_0}$.

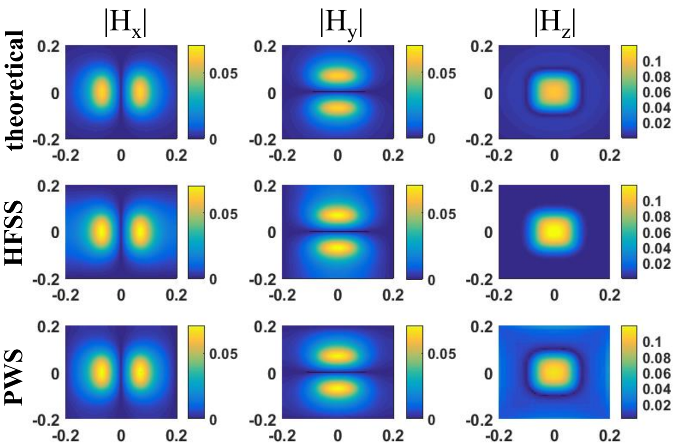

Fig. 6. Comparison between theoretical, simulated, and calculated magnetic field profiles at z=5cm above the DUT (colorbar unit: A/m)

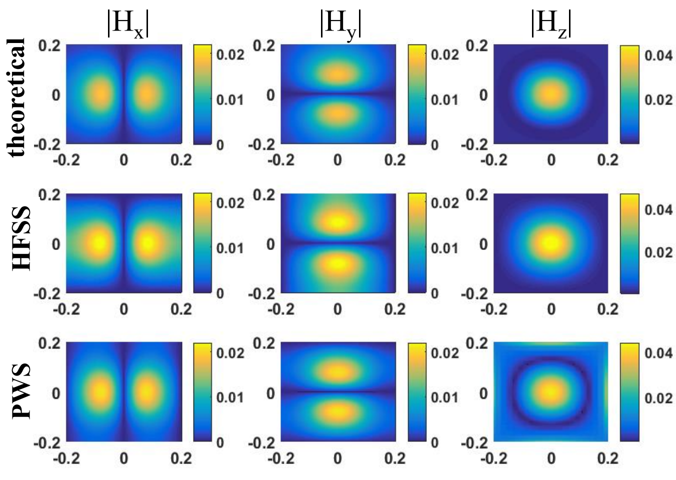

Fig. 7. Comparison between theoretical, simulated, and calculated magnetic field profiles at z=10cm above the DUT (colorbar unit: A/m)

V. Conclusion

In this paper, we present the PWS method applied on the near-filed characterization above an RFID reader antenna operating at 13.56 MHz. This algorithm was computed to extract the 3D magnetic field components from the tangential ones at an initial plane that is 1 cm above the antenna under test. Also the extraction of the magnetic field components at 5 and 10 cm above the DUT was performed. The theoretical calculations of the magnetic field were performed and compared, with the simulated ones, to the extracted values from the proposed algorithm. The validity of the methods was shown with a good agreement between the calculations, electromagnetic simulations, and the theoretical quantities.

Acknowledgment

This research work was done at PHELINE, a test lab common with CSTB and Grenoble Alpes University. It is specialized in the study of the electromagnetic fields phenomenon and its interactions with the environment. This work was supported by ANSES - French Agency for Food, Environmental and Occupational Health & Safety.

References

[1] W.-J. Zhao, B.-F. Wang, E.-X. Liu, H. B. Park, H. H. Park, E. Song, and E.-P. Li, "An Effective and Efficient Approach for Radiated Emission Prediction Based on Amplitude-Only Near-Field Measurements," IEEE Trans. Electromagn. Compat., vol. 54, no. 5, pp. 1186-1189, Oct. 2012.

[2] W.-J. Zhao, B. Wang, E.-X. Liu, H. B. Park, H. H. Park, S. Eakhwan, and E.-P. Li, "A differential evolution based equivalent source approach for predicting electromagnetic emissions using near-field scanning," in Proc. IEEE Int. Symp. Electromagn. Compat., Denver, CO, Aug. 2013, pp. 182-186.

[3] WANG J.J.H. : 'An examination of the theory and practices of planar near-field measurement', IEEE Trans. Antennas Propag., 1988, 36, (6), pp. 746–753

[4] T. Ordas, M. Lisart, E. Sicard, P. Maurine and L. Torres, "Near-field mapping system to scan in time domain the magnetic emissions of integrated circuits," Proc. PATMOS' 08: Int. Workshop on Power and Timing Modeling Optimization and Simulation, Ver. 1-11, 2009

[5] K. Jomaa, F. Ndagijimana, J. Jomaah, H. Ayad, "Near-field Measurement System with 3D Magnetic-field Probe Design for Dosimetric Applications", Middle East Conference on Antennas and Propagation (MECAP), Sep. 2016.

[6] T. Stadtler, L. Eifler and J. L. Ter Haseborg, "Double probe near field scanner, a new device for measurements in time domain," Proc of IEEE Int. Symp. EMC TU, Hamburg-Harburg, Hamburg, Germany, pp. 86-90, 1, Aug. 2003.

[7] K. Jomaa, N. Sivaraman, F. Ndagijimana, H. Ayad, M. Fadllallah, J. Jomaah, "Development of a 3D Scanning System for Magnetic Near-field Characterization" Proc of IEEE International Symposium on Electromagnetic Compatibility & Signal/Power Integrity (EMCSI), Washington-DC, USA, pp. 492-497, Aug. 2017

[8] R. C. RUDDUCK, D. C. F. RTJ, AKD M. R. INTIHAR "Near-Field Analysis by the Plane-Wave Spectrum Approach" IEEE Transactions on Antenna and Propagation, pp. 231-234 March 1973.

[9] P. C. CLEMMOW "The Plane Wave Spectrum Representation of Electromagnetic Fields" First edition, IEEE Press, 1966.

[10] Burdette E., "Plane Wave Analysis of Near-zone Fields Using Wavenumber Band-pass Filtering" Thesis, Georgia Institute of Technology, May 1976

[11] Balanis, C. A., "Antenna Theory Analysis and Design, 2nd Ed.", John Wiley & Sons, New York, 1997.

[12] G. Viziteu, B. Florean, G.M. Moraru, and A. Pintea, "An Overview of RFID Technology Used In Library", International Conference and Exposition on Electrical and Power Engineering (ICEPE), 2012, pp. 108-111